# Supplementary Information

## H/F isosteric substitution to attest different equi-energetic molecular conformations in crystals

*Amol G. Dikundwar,[a] Ch. Venkateswarlu,[b] R. N. Chandrakala,[b] Srinivasan Chandrasekaran*[b] and Tayur N. Guru Row*[a]*

[a]Solid State and Structural Chemistry Unit, Indian Institute of Science, Bangalore, 560 012, India
Email: ssctng@sscu.iisc.ernet.in
[b]Department of Organic Chemistry, Indian Institute of Science, Bangalore 560012, India
Email: scn@orgchem.iisc.ernet.in

---

## Index



### Figures



### Tables

# Synthesis and characterization of compounds 1–6

All reagents and solvents were purchased from Sigma–Aldrich, Alfa Aesar and were used as supplied unless otherwise stated. All reactions were performed in oven dried apparatus and were stirred magnetically. Infrared spectra were recorded using the JASCO FT–IR instrument and the frequencies are reported in wave numbers ($cm^{-1}$) and intensities of the peaks are denoted as s (strong), w (weak), m (medium). $^{1}H$ and $^{13}C$ NMR spectra were recorded on Jeol 400 MHz (100 MHz, $^{13}C$) NMR spectrometer and calibrated using residual undeuterated solvent as an internal reference. $^{19}F$ NMR spectra (Proton decoupled) were recorded on a Bruker 400 MHz (376 MHz, $^{19}F$) spectrometer and calibrated using trichlorofluoromethane as an external reference. Chemical shifts are reported in parts per million and multiplicity is indicated using the following abbreviations: s (singlet), d (doublet), t (triplet), q (quartet), m (multiplet), sb (broad singlet) and db (broad doublet). Mass spectra were recorded on a Q–TOF electrospray instrument. Melting points reported are uncorrected. All the spectra were recorded in $CDCl_3$ unless mentioned otherwise.

## Preparation of Hex–2,4–diyne–1,6–bisoxycarbonyl chloride

To a stirred solution of Hex–2,4–diyne–1,6–diol[1] (0.5g, 4.5 mmol) in dry ether (40 ml) at 0 °C, triphosgene (1.35g, 4.5 mmol) was added and stirred for 30 min. To this solution activated charcoal (0.05g) was added at 0 °C and stirred for 12 h at room temperature (28 °C).The resultant solution was filtered on celite pad. The ether layer was concentrated under reduced pressure and the remaining liquid was used for reactions without any further purification.

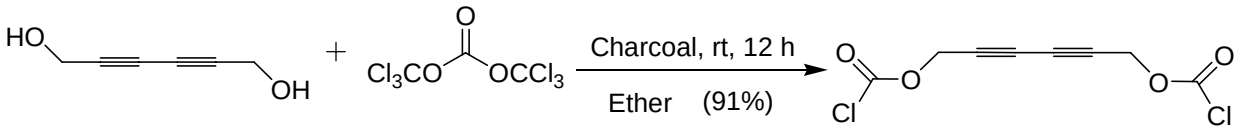


**Physical state:** pale yellow liquid
**FTIR (KBr):** 2167(w), 1778(s), 1359(m), 1129(s)
**$^{1}H$ NMR**: δ 4.96 (s)
**$^{13}C$ NMR:** δ 150.85, 72.76. 72.66, 59.04

1. Y. Weiyan, H. Chuan, C. Mao, Z. Heng, L. Aiwen, *Org. Lett.*, 2009, **11**, 709.

## General procedure for the synthesis of symmetrical diacetylenic bis–carbonates, 1–6

To a solution of aryl alcohol (2 eq) in anhydrous dichloromethane (20 ml) at –10 °C, triethylamine (0.83 ml, 5.99 mmol, 2.2 eq) was added drop wise. The solution was stirred for 10 min and hex–2,4–diyne–1,6–bisoxycarbonyl chloride (0.64 g, 2.72 mmol, 1 eq) was added over a period of 10 min and stirred at this temperature for 1h. The reaction mixture was allowed to attain room temperature. After 4h, the reaction mixture was diluted with dichloromethane (30 ml), water (2×15 ml) and brine solution (15 ml). The organic layer was dried over anhydrous $Na_2SO_4$ and the products were purified by column chromatography on silica gel (230–400 mesh) using the eluting solution of 5% ethyl acetate in hexane. Recrystallization with DCM and pet ether afforded the products as white crystalline solids (percentage yields ~70-80).

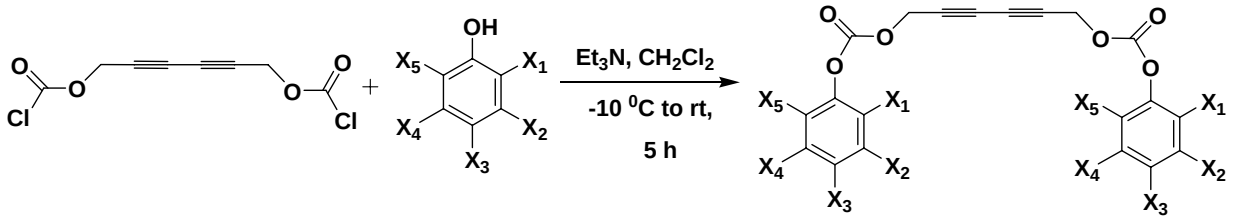


**1, X=H**
**2, X2=X3=X4=X5=H, X1=F**
**3, X1=X3=X4=X5=H, X2=F**
**4, X1=X2=X4=X5=H, X3=F**
**5, X2=X4=H, X1=X3=X5=F**
**6, X=F**

**Compound 1**

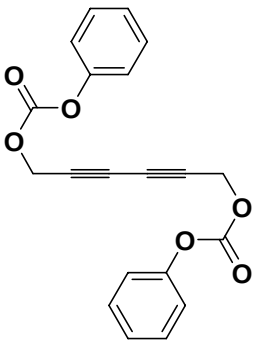

**Physical state:** White crystalline solid
**Melting point:** 109 °C
**FTIR (KBr):** 1769(s), 1269(m), 1231(s), 1203(s)
**$^1$H NMR (400 MHz, $CDCl_3$)**: δ 7.42–7.37 (m, 2H), 7.28–7.18 (m, 3H), 4.92 (s, 2H)
**$^{13}$C NMR (100 MHz, $CDCl_3$):** δ 152.94, 150.89, 129.53, 126.29, 120.85, 72.99, 71.31, 56.09
**High resolution ESMS (m/z):** Calculated for $C_{20}H_{14}O_6$+Na: 373.0688
Observed: 373.0701

**Compound 2**

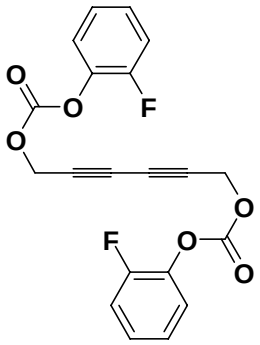

**Physical state:** White crystalline solid
**Melting point:** 98 °C
**FTIR (KBr):** 1778(s), 1502(m), 1230(s), 1179(m)
**$^{1}$H NMR (400 MHz, $CDCl_3$)**: δ 7.27–7.14 (m, 4H), 4.95 (s, 2H)
**$^{13}$C NMR (100 MHz, $CDCl_3$):** δ 153.83 (d, $J_{CF}$ = 248.6), 152.10, 138.32 (d, $J_{CF}$ = 12.3), 127.64 (d, $J_{CF}$ = 7.1), 124.52 (d, $J_{CF}$ = 3.9), 123.16, 116.90 (d, $J_{CF}$ = 18.2), 72.81,71.46, 56.57
**$^{19}$F NMR (376 MHz, $CDCl_3$):** δ –129.12
**High resolution ESMS (m/z):** Calculated for $C_{20}H_{12}F_2O_6$+Na: 409.0500
Observed: 409.0500

**Compound 3**

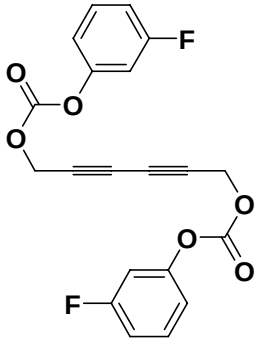

**Physical state:** White crystalline solid
**Melting point:** 88 °C
**FTIR (KBr):** 1769(s), 1267(s), 1247(s)
**$^{1}$H NMR (400 MHz, $CDCl_3$)**: δ 7.39–7.33 (m, 1H), 7.02–6.97 (m, 3H), 4.93 (s, 2H)
**$^{13}$C NMR (100 MHz, $CDCl_3$):** δ 162.73 (d, $J_{CF}$ = 246.6), 152.46, 151.52 (d, $J_{CF}$ = 10.7), 130.30 (d, $J_{CF}$ = 9.4), 116.62 (d, $J_{CF}$ = 3.3), 113.38 (d, $J_{CF}$ = 20.7), 109.07 (d, $J_{CF}$ = 24.8), 72.88, 71.41, 56.25
**$^{19}$F NMR (376 MHz, $CDCl_3$):** δ –110.39
**High resolution ESMS (m/z):** Calculated for $C_{20}H_{12}F_2O_6$+Na: 409.0500
Observed: 409.0504

**Compound 4**

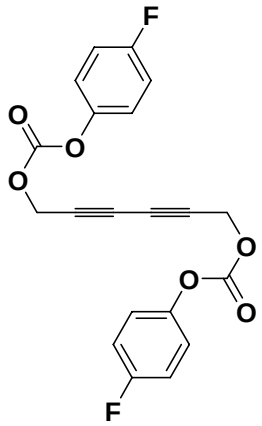

**Physical state:** White crystalline solid
**Melting point:** 126 °C
**FTIR (KBr):** 1774(s), 1505(s), 1228(s), 1190(m)
**$^{1}$H NMR (400 MHz, $CDCl_3$)**: δ 7.18–7.14 (m, 2H), 7.10–7.05 (m, 2H), 4.91 (s, 2H)
**$^{13}$C NMR (100 MHz, $CDCl_3$):** δ 160.41 (d, $J_{CF}$ = 243.6), 152.96, 146.76 (d, $J_{CF}$ = 2.6 ), 122.36 (d, $J_{CF}$ = 8.7), 116.20 (d, $J_{CF}$ = 23.2), 72.96,71.37, 56.20
**$^{19}$F NMR (376 MHz, $CDCl_3$):** δ –116.05
**High resolution ESMS (m/z):** Calculated for $C_{20}H_{12}F_2O_6$+Na: 409.0500
Observed: 409.0505

**Compound 5**

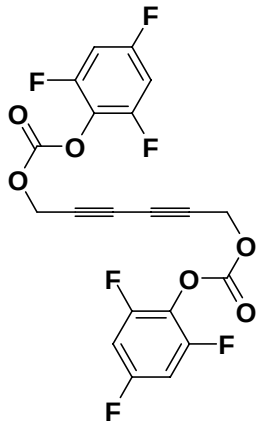

**Physical state:** White crystalline solid
**Melting point:** 94 °C
**FTIR (KBr):** 1777(s), 1511(m), 1260(s), 1215(s), 1048(s)
**$^{1}$H NMR (400 MHz, $CDCl_3$)**: δ 6.82–6.75 (m, 2H), 4.97 (s, 2H)
**$^{13}$C NMR (100 MHz, $CDCl_3$):** δ 159.70 (dt, $J_{CF}$ = 248.4, 13.6,), 155.06 (ddd, $J$ = 251.3, 15.0, 5.6), 151.35, 124.47 (td, $J$ = 16.1, 5.5), 101.27–100.74 (m), 72.44, 71.70, 57.15
**$^{19}$F NMR (376 MHz, $CDCl_3$):** δ –109.15 (t, $J$ = 4.1), –122.96 (d, $J$ = 4.5)
**High resolution ESMS (m/z):** Calculated for $C_{20}H_8F_6O_6$+Na: 481.0123
Observed: 481.0125

**Compound 6**

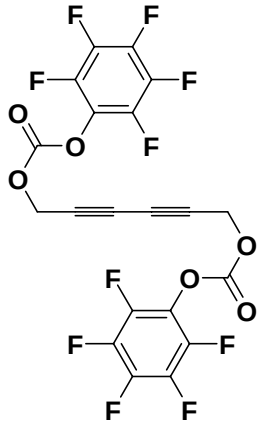

**Physical state:** White crystalline solid
**Melting point:** 85–86 °C
**FTIR (KBr):** 1798(s), 1524(s), 1222(s), 980(s)
**$^{1}$H NMR**: δ 4.99 (s)
**$^{13}$C NMR:** δ 150.8, 72.3, 72.0, 57.7
**$^{19}$F NMR:** δ –152.93 (d, 2F), –156.85 (t, 1F), –161.72 (m, 2F)
**High resolution ESMS (m/z):** Calculated for $C_{20}H_4F_{10}O_6$+Na: 552.9746
Observed: 552.9741

**Reference:** A G. Dikundwar, Ch. Venkateswarlu, R. O. Piltz, S. Chandrasekaran, T. N. Guru Row, *CrystEngComm*, 2011, **13**, 1531.

# X-ray crystallography

X-ray diffraction datasets were collected on an Oxford Xcalibur (Mova) diffractometer[1] equipped with a Eos CCD detector using MoKα radiation (λ= 0.71073Å). The crystals were maintained at the desired temperature during data collection using the Oxford Instruments Cryojet–HT controller.[2] All structures were solved by direct methods using SHELXS–97 and refined against $F^2$ using SHELXL–97.[3] H-atoms were fixed geometrically and refined isotropically. The WinGX package[4] was used for refinement and production of data tables. All *ORTEP* representations and packing diagrams were made using MERCURY[5] or CAMERON.[6] Analysis of the H–bonded and pi–interactions was carried out using PLATON[7] for all the structures.

**Table S1** Crystal data of compounds **1**–**6**

| **DATA** | **1** | **2** | **3** | **4** | **5** | **6** |
|---|---|---|---|---|---|---|
| CCDC number | 759062 | 922274 | 922273 | 922275 | 922272 | 784071 |
| Formula | $C_{20}H_{14}O_6$ | $C_{20}H_{12}F_2O_6$ | $C_{20}H_{12}F_2O_6$ | $C_{20}H_{12}F_2O_6$ | $C_{20}H_8F_6O_6$ | $C_{20}H_4F_{10}O_6$ |
| Formula weight | 350.31 | 386.30 | 386.30 | 386.30 | | 530.23 |
| Color | Colourless | Colourless | Colourless | Colourless | Colourless | colorless |
| Crystal morphology | Block | Block | Needle | Block | Block | Needle |
| Crystal size (mm) | 0.40 0.20 0.20 | 0.40 0.20 0.20 | 0.40 0.10 0.10 | 0.40 0.20 0.20 | 0.30 0.25 0.20 | 0.30 0.12 0.12 |
| Temperature/K | 150(1) | 150(1) | 150(1) | 150(1) | 150(1) | 150(1) |
| Radiation | Mo Kα | Mo Kα | Mo Kα | Mo Kα | Mo Kα | Mo Kα |
| Wavelength/Å | 0.71073 | 0.71073 | 0.71073 | 0.71073 | 0.71073 | 0.71073 |
| Crystal system | Orthorhombic | Orthorhombic | Monoclinic | Orthorhombic | Triclinic | Monoclinic |
| Space group | *Pccn* | *Pccn* | $P2_1/n$ | *Pccn* | *P*–1 | $P2_1/c$ |
| *a* (Å) | 9.5387(15) | 9.9560(50) | 20.8305(12) | 9.6359(9) | 5.2422(3) | 5.8951(9) |
| *b* (Å) | 23.2080(36) | 22.6650(50) | 3.9051(3) | 23.7478(21) | 7.1560(4) | 10.1943(16) |
| *c* (Å) | 7.4056(12) | 7.4420(50) | 22.4954(12) | 7.2680(6) | 13.2155(7) | 17.245(2) |
| *α* (°) | 90 | 90 | 90 | 90 | 93.426(4) | 90 |
| *β* (°) | 90 | 90 | 110.433(7) | 90 | 98.645(4) | 108.115(5) |
| *γ* (°) | 90 | 90 | 90 | 90 | 109.868(5) | 90 |
| Volume (Å$^3$) | 1639.41(4) | 1679.31(15) | 1714.78(44) | 1663.15(3) | 457.66(10) | 985.0(2) |
| Z | 4 | 4 | 4 | 4 | 1 | 2 |
| Density (g/ml) | 1.41 | 1.52 | 1.49 | 1.54 | 1.66 | 1.788 |
| *μ* (1/mm) | 0.106 | 0.128 | 0.125 | 0.129 | 0.161 | 0.191 |
| F (000) | 728 | 792 | 792 | 792 | 230 | 524 |
| *θ* (min, max) | 1.7, 26.3 | 3.3, 25.0 | 2.7, 25.0 | 1.7, 25.0 | 3.0, 25.0 | 2.3, 26.0 |
| No. Unique Reflns | 1674 | 1480 | 3031 | 1731 | 1614 | 1937 |
| No. of parameters | 118 | 127 | 253 | 166 | 145 | 171 |
| $h_{min,max}$ | –11, 11 | –11, 11 | –24, 24 | –11, 11 | –6, 6 | –7, 7 |
| $k_{min,max}$ | –29, 29 | –26, 25 | –4, 4 | –28, 28 | –8, 8 | –12, 12 |
| $l_{min,max}$ | –9, 9 | –8, 8 | –26, 26 | –6, 8 | –15, 15 | –21, 21 |
| $R_{all}$, $wR_{2\ all}$ | 0.041, 0.081 | 0.050, 0.100 | 0.044, 0.103 | 0.050, 0.109 | 0.031, 0.074 | 0.067, 0.120 |
| $R_{obs}$, $wR_{2\ obs}$ | 0.030, 0.077 | 0.037, 0.092 | 0.036, 0.097 | 0.037, 0.101 | 0.029, 0.073 | 0.050, 0.114 |
| $\Delta\rho_{min}$, $\Delta\rho_{max}$ (eÅ$^{-3}$) | –0.18, 0.18 | –0.18, 0.19 | –0.22, 0.16 | –0.21, 0.23 | –0.20, 0.19 | –0.18, 0.26 |
| GooF | 1.04 | 1.06 | 1.05 | 1.04 | 1.02 | 1.15 |

**References:**


1. Oxford Diffraction (2009). *CrysAlis PRO CCD* and *CrysAlis PRO RED*. Agilent Technologies Ltd, Santa Clara, CA, USA.
2. Oxford instruments, Cryojet XL/HT controller, Oxford Diffraction Ltd, Yarnton, England.
3. G. M. Sheldrick, *Acta Crystallogr., Sect. A: Found. Crystallogr.* 2008, **64**, 112.
4. L. J. Farrugia, *J. Appl. Crystallogr.*, 1999, **32**, 837.
5. C. F. Macrae, P. R. Edgington, P. McCabe, E. Pidcock, G. P. Shields, R. Taylor, M. Towler, J. van de Streek, *J. Appl. Cryst.* 2006, **39**, 453.
6. D. J. Watkin, C. K. Prout and L. J. Pearce, (1996), *CAMERON*. Chemical Crystallography Laboratory, Oxford, England.
7. A. L. Spek, *J. Appl. Crystallogr.*, 2003, **36**, 7.

**Table S2** Intermolecular interactions in the crystal structures of compounds **1**–**6**

| D–H···A | r(D–H)/Å | r(D–A)/Å | r(H···A)/Å | ∠ D–H···A/º | Symmetry |
|---|---|---|---|---|---|
| **1** | | | | | |
| C3–H3A···O1 | 0.97 | 3.530(1) | 2.759(1) | 136.9(1) | x,–y+1/2+1,+z–1/2 |
| C3–H3A···O3 | 0.97 | 3.575(1) | 2.997(1) | 119.4(2) | x,–y+1/2+1,+z–1/2 |
| C3–H3B···Cg(1) | 0.97 | 3.581 (1) | 2.669 | 155 | x,y,1+z |
| **2** | | | | | |
| C3–H3A···O1 | 0.97 | 3.498(2) | 2.729(1) | 136.5(2) | x,-y+1/2,+z-1/2 |
| C9–H9···O2 | 0.93 | 3.325(3) | 2.501(2) | 147.7(1) | -x+1/2,+y,+z+1/2 |
| C3–H3A···O3 | 0.97 | 3.493(2) | 2.920(1) | 118.8(2) | x,-y+1/2,+z-1/2 |
| C7–H7···O2 | 0.93 | 3.571(2) | 2.995(1) | 121.5(1) | -x,-y,-z+1 |
| C8–H8···F1 | 0.93 | 3.534(2) | 2.658(1) | 157.2(1) | x+1/2,-y,-z+1/2+1 |
| C3–H3B···F1 | 0.97 | 3.462(2) | 2.897(1) | 118.1(2) | -x-1/2,+y,+z-1/2 |
| C3–H3B···Cg(1) | 0.97 | 3.561(3) | 2.670 | 153 | x,y,-1+z |
| **3** | | | | | |
| C3–H3B···O1 | 0.97 | 3.410(2) | 2.472(1) | 162.6(2) | x,+y–1,+z |
| C6'–H6'···O3' | 0.93 | 3.447(2) | 2.547(1) | 162.8(1) | –x+1/2,y+1/2,–z+1/2 |
| C6'–H6'···O1' | 0.93 | 3.343(2) | 2.560(1) | 142.0(1) | –x+1/2,y+1/2, -z+1/2 |
| C8–H8···O2' | 0.93 | 3.483(2) | 2.578(1) | 164.4(1) | –x+1/2,y–1/2,–z+1/2 |
| C3'–H3'2···O1' | 0.97 | 3.500(2) | 2.585(1) | 157.3(1) | x,+y+1,+z |
| C10–H10···O1 | 0.93 | 3.474(2) | 2.654(1) | 147.5(1) | –x+1/2,y–1/2,–z+1/2 |
| C10'–H10'···O2' | 0.93 | 3.309(2) | 2.722(1) | 121.8(1) | x,+y–1,+z |
| C6–H6···O2 | 0.93 | 3.375(2) | 2.730(1) | 127.2(1) | x,+y+1,+z |
| C3'–H3'1···O2 | 0.97 | 3.409(2) | 2.753(1) | 125.4(1) | –x+2,–y+2,–z+2 |
| C10–H10···O3 | 0.93 | 3.751(3) | 2.840(1) | 166.4(1) | –x+1/2,y–1/2,–z+1/2 |
| C8'–H8'···F1 | 0.93 | 3.344(2) | 2.631(1) | 133.9(1) | x–1/2,-y+1/2,z+1/2 |
| C10'–H10'···F1 | 0.93 | 3.453(2) | 2.919(1) | 117.8(1) | –x+1/2,y–1/2,–z+1/2 |
| C9'–H9'···F1 | 0.93 | 3.328(2) | 2.639(1) | 131.4(1) | –x+1/2,y–1/2,–z+1/2 |
| C3'–H3'1···F1' | 0.97 | 3.509(2) | 2.921(1) | 120.0(1) | –x+1/2,y–1/2,–z+1/2 |
| **4** | | | | | |
| C10–H10···F1 | 0.93 | 3.192(2) | 2.594(1) | 122.5(2) | x+1/2,–y+1,–z–1/2 |
| C9–H9···F1 | 0.93 | 3.201(2) | 2.614(1) | 121.6(2) | x+1/2,–y+1,–z–1/2 |
| C9–H9···F1 | 0.93 | 3.428(2) | 2.865(1) | 120.1(1) | –x+1,–y+1,–z–1 |
| C7–H7···O2 | 0.93 | 3.297(2) | 2.468(1) | 148.5(1) | –x+1/2,+y,+z–1/2 |
| C3–H3B···O1 | 0.97 | 3.469(2) | 2.690(1) | 137.6(1) | x,–y+1/2,+z+1/2 |
| C3–H3A···Cg(1) | 0.97 | 3.605(2) | 2.690 | 157 | –x+1,–y+1,–z–1 |
| **5** | | | | | |
| C3–H3B···O2 | 0.97 | 3.229(2) | 2.420(1) | 140.6(1) | –x,–y+1,–z |
| C3–H3B···O1 | 0.97 | 3.494(2) | 2.818(1) | 127.4(1) | –x+1,–y+1,–z |
| C3–H3A···F3 | 0.97 | 3.243(2) | 2.431(1) | 141.0(1) | x,+y+1,+z |
| C9–H9···F1 | 0.93 | 3.269(2) | 2.479(1) | 142.8(1) | x,+y–1,+z |
| C7–H7···F2 | 0.93 | 3.403(2) | 2.528(1) | 156.9(2) | –x–1,–y,–z+1 |
| C7–H7···F1 | 0.93 | 3.387(2) | 2.762(1) | 125.4(1) | –x,–y+1,–z+1 |
| **6** | | | | | |
| C3–H2A···O2 | 0.99(3) | 3.435(3) | 2.49(2) | 157(2) | x+1,+y,+z |
| C3–H2B···F4 | 0.92(2) | 3.636(3) | 2.84(2) | 145(2) | x,–y–1/2,+z–1/2 |
| C3–H2B···F5 | 0.92(2) | 3.362(3) | 2.90(2) | 111(1) | –x–1,y+1/2,–z–1/2–1 |

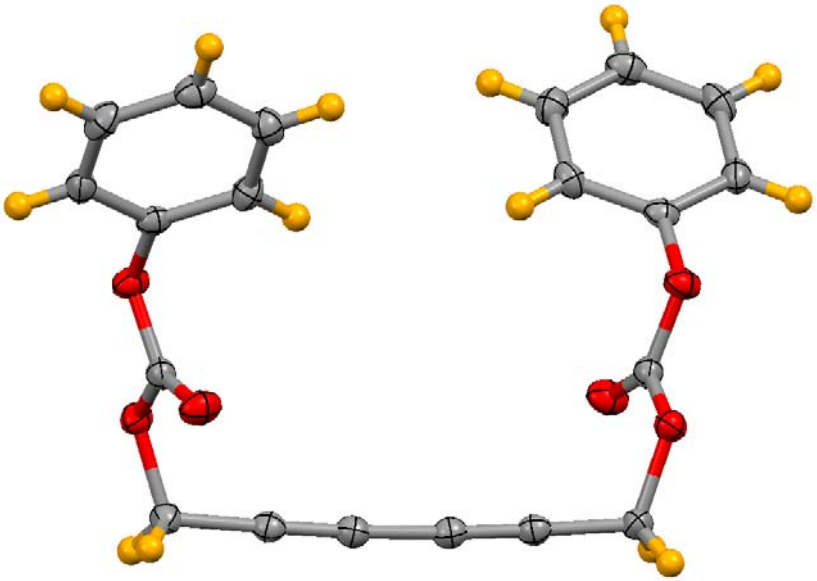

**(a)**

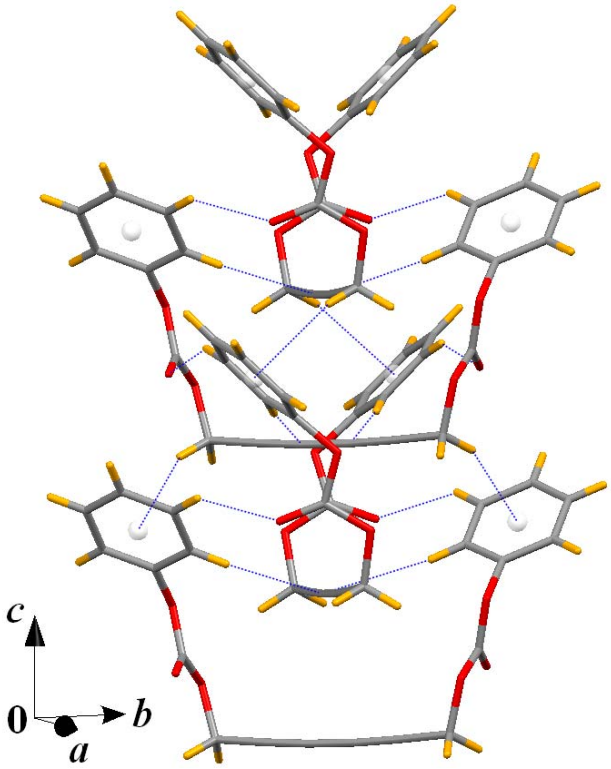


**(b)**

**Figure S1** (a) ORTEP (50 % probability ellipsoids) and (b) packing diagram of compound 1

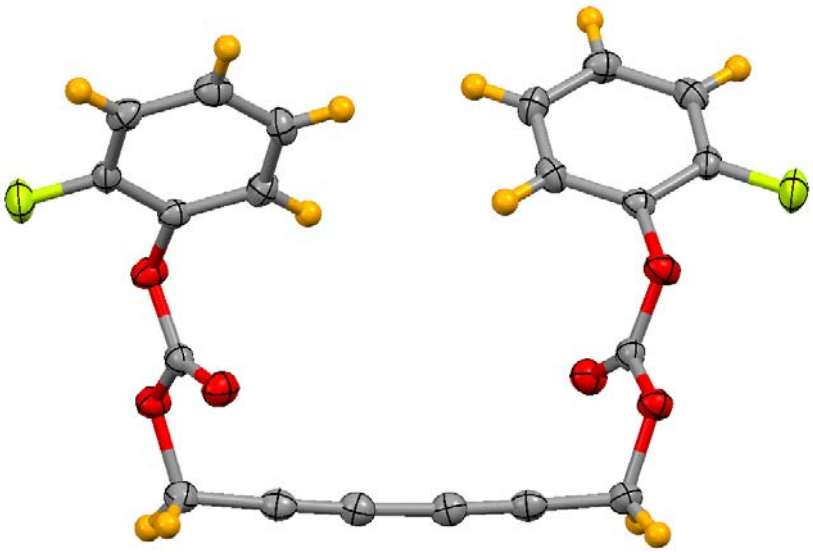

**(a)**

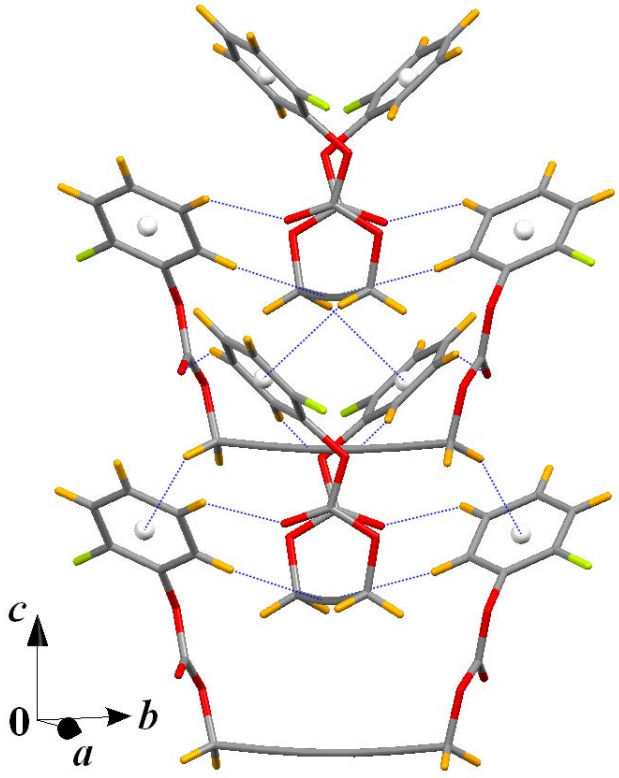


**(b)**

**Figure S2** (a) ORTEP (50 % probability ellipsoids) and (b) packing diagram of compound 2

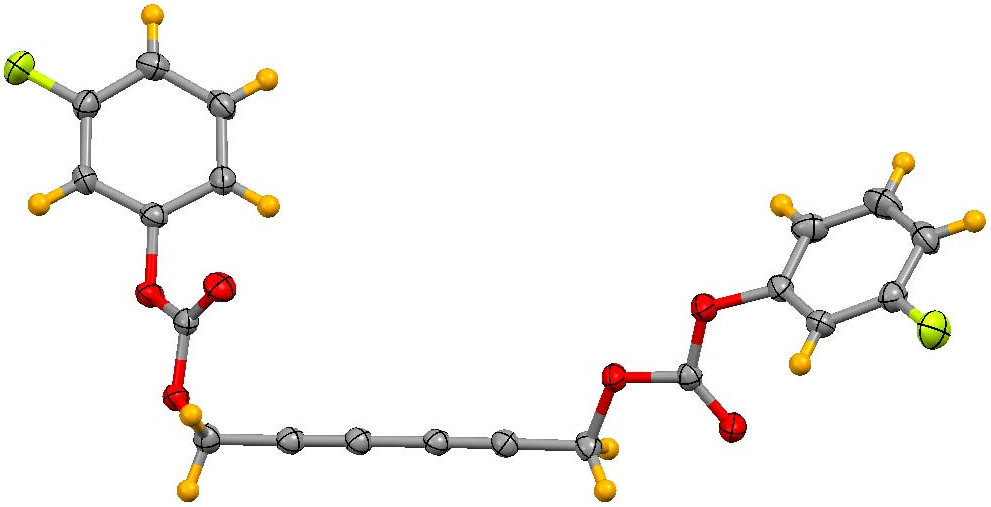

**(a)**

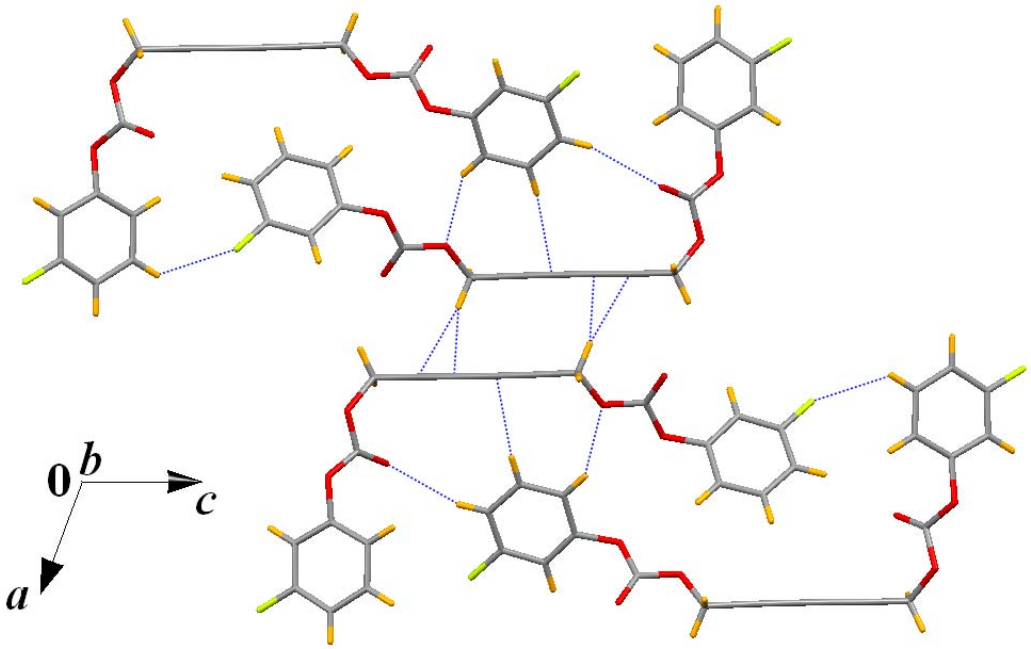


**(b)**

**Figure S3** (a) ORTEP (50 % probability ellipsoids) and (b) packing diagram of compound 3

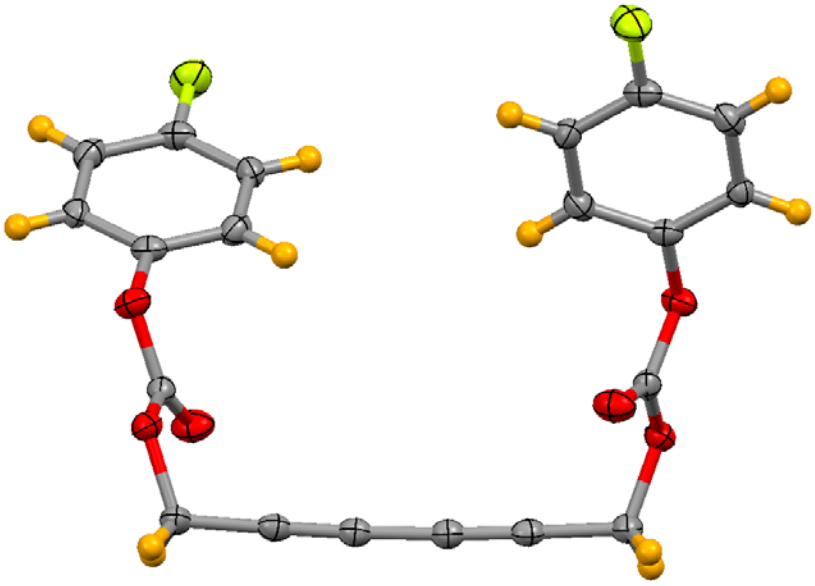

**(a)**

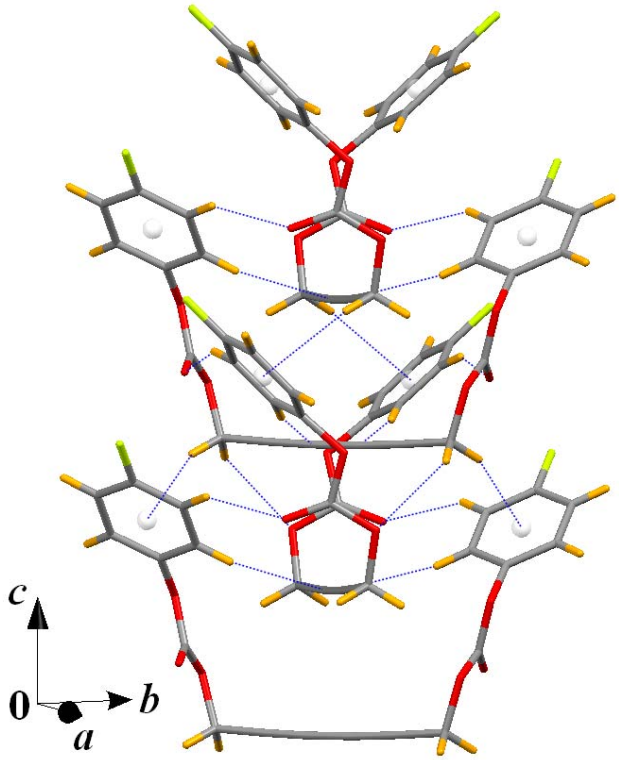


**(b)**

**Figure S4** (a) ORTEP (50 % probability ellipsoids) and (b) packing diagram of compound 4

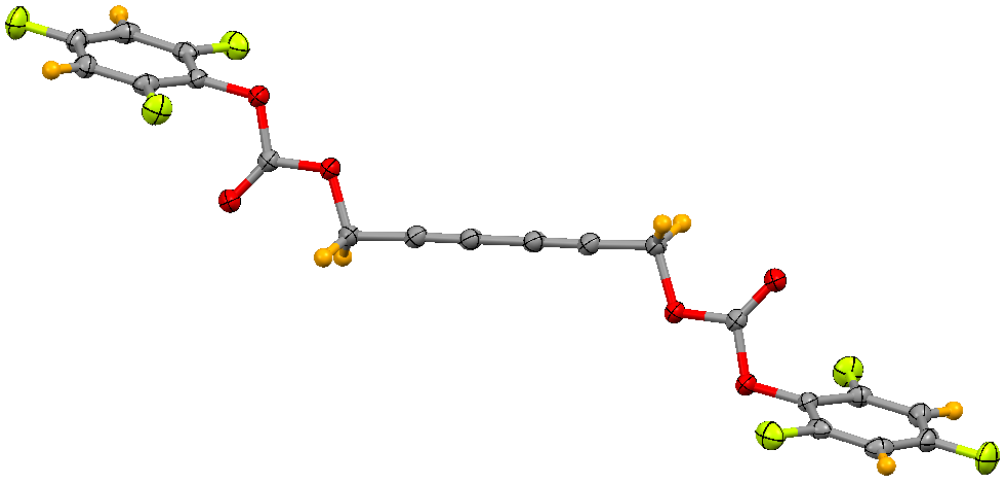

**(a)**

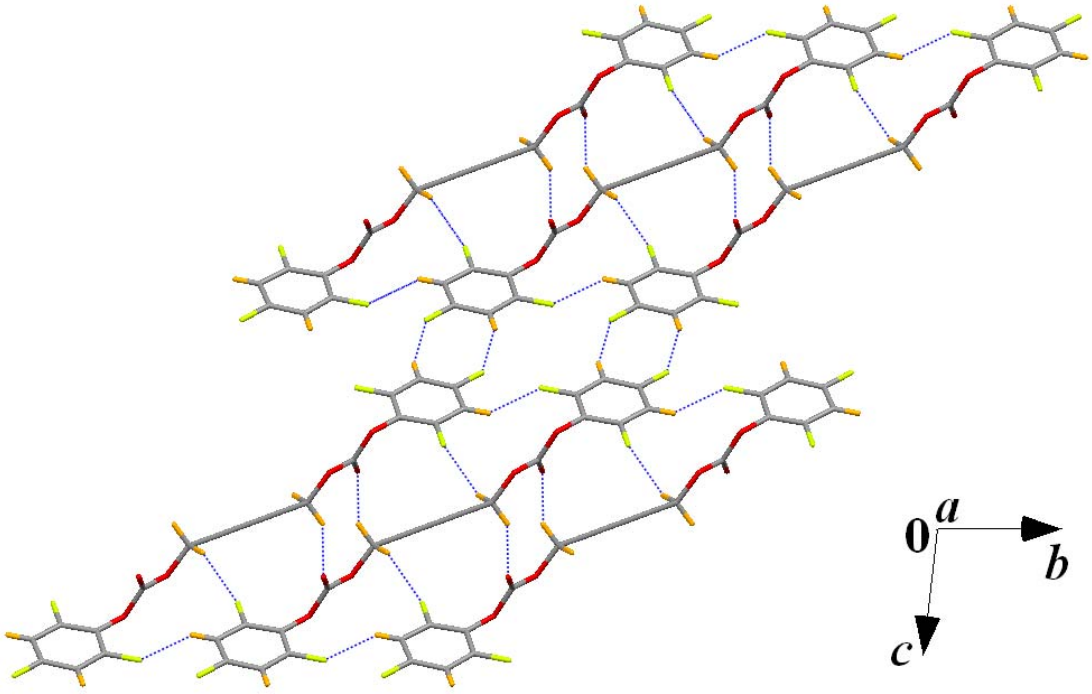


**(b)**

**Figure S5** (a) ORTEP (50 % probability ellipsoids) and (b) packing diagram of compound 5

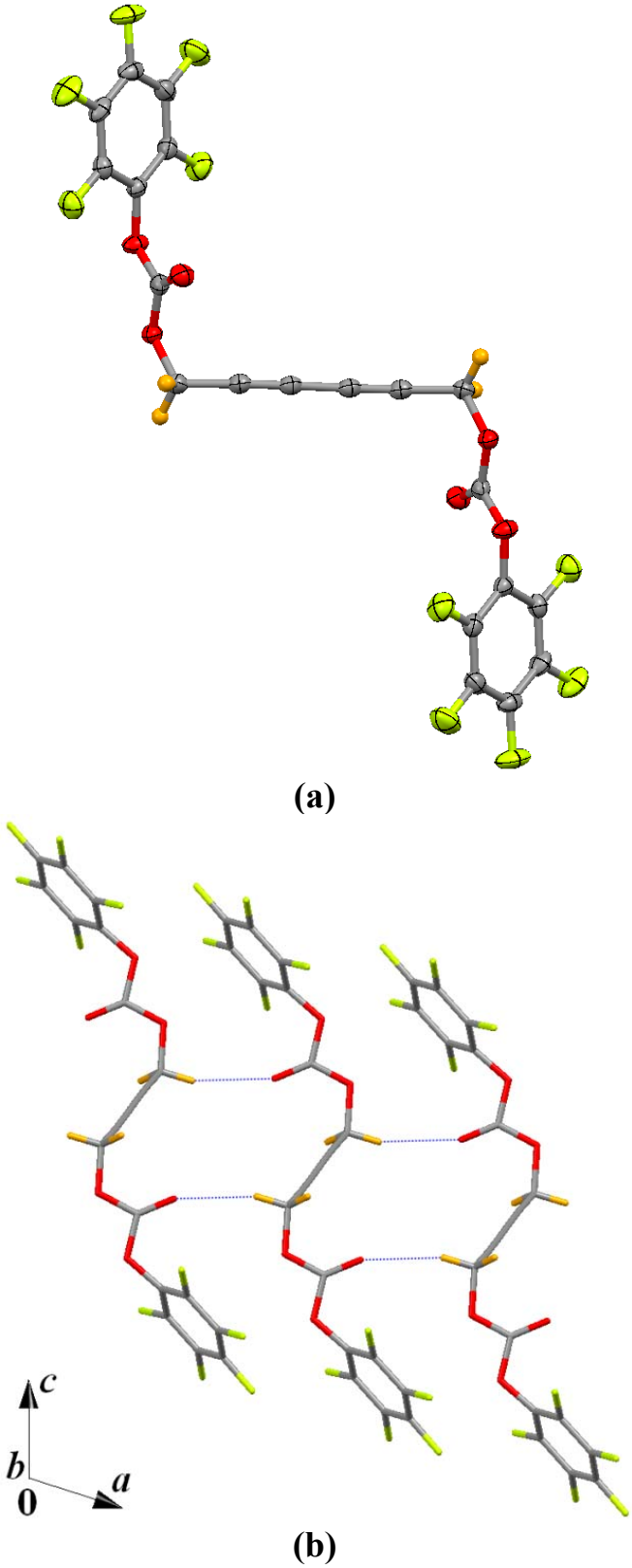


**Figure S6** (a) ORTEP (50 % probability ellipsoids) and (b) packing diagram of compound 6

## Possible reasoning for different molecular conformation of compound 3 from that of compounds 1, 2 and 4 based on supramolecular packing patterns in crystals

As explained in the manuscript, the twisted conformations of molecules **1**, **2** and **4** have been mainly attributed to the availability of free meta C–H groups involved in the (ph)$C_{meta}$–H···O=C hydrogen bonding as observed in their respective crystal structures. In compound **3**, one of the two C–H groups is available for the formation of a (ph)$C_{meta}$–H···O=C hydrogen bond while the other is fluoro substituted (C–F) and hence, assuming the equi-volume relationship of H and F, orientation of the ring will have an effect on the availability of a meta C–H group to be involved in the (ph)$C_{meta}$–H···O=C hydrogen bond. In compound **5**, although both the meta C–H groups are present, the molecule differs completely in its electronic properties ($\pi$ to $\pi_F$) and steric properties due to trifluoro substitution. Further, the gas phase optimized geometry of **5** is also anti ($\varphi$ = 180°) as that observed in its crystalline state where both the meta C–H groups are involved in the C–H···F interactions (figure S5(b)).

Additionally, upon close inspection of the structures, it has been noticed that in compound **1**, the intermolecular distance between the two meta H-atoms [(meta)H···H(meta)], one involved in (ph)$C_{meta}$–H···O=C and another free H, is considerably short, 2.416 Å (sum of vander Waals radii of H is 2.4 Å) whereas, there are no such close contacts for hydrogens at ortho and para position. As a result, when an F atom is substituted at ortho or para position of **1**, the 3D packing pattern with (ph)$C_{meta}$–H···O=C and $C_{sp3}$–H···$\pi$ can still be retained with similar molecular conformation giving rise to the isostructural crystals of **1**, **2** and **4**. The corresponding (meta)H···H(meta) distance in **2** is again very short (2.394 Å) whereas, in **4**, the free meta hydrogen gets involved in the favorable C–H···F hydrogen bond with the C–F group at para position (see figures below). When one of the meta position of **1** is substituted by F, if the ensuing crystal structure were to be similar to that of **1**, **2** and **4** with (ph)$C_{meta}$–H···O=C hydrogen bond, there may be a steric crowding of (meta)H and F(meta) oriented unfavourably for the formation of (meta)C–H···F–C(meta) hydrogen bond (i. e. $\angle$ C–H···F $\approx$ 90° and $\angle$ H···F–C $\approx$ 180°). So, with similar molecular conformation (cisoid) if the meta F-substituted compound i.e. **3** favours (meta)C–H···O=C then (meta)C–H···F–C(meta) gets unfavoured and if the phenyl ring were to flip 180° to favor (meta)C–H···F–C(meta) [with $\angle$ C–H···F $\approx$ 180° and $\angle$ H···F–C $\approx$ 90°)], the (meta)C–H···O=C cannot form. Consequently, **3** prefers to adopt a non-symmetric conformation (unlike **1**, **2** and **4** which are dissymmetric) where it can maximize the formation of C–H···F, C–H···O and C–H···$\pi$ interactions as shown in the packing diagram (figure S3(b)).

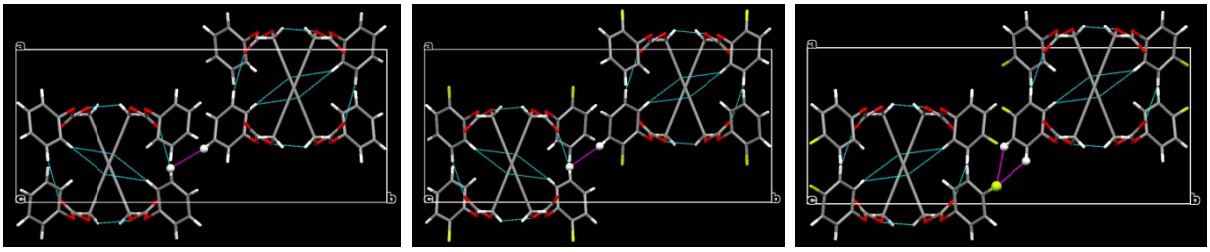

Packing diagrams showing (meta)H···H(meta) in **1** [2.41(1) Å]; (meta)H···H(meta) in **2** [2.39(1) Å] and (ortho/meta)C–H···F–C(para) in **4** [2.594(2)/2.614(2)Å] .

Despite of above reasoning with respect to supramolecular packing, it must be noted that gas phase geometry optimization of **3** also suggest a "*gauche*" conformation (φ=104°) in contrast with the cisoid (φ≈9°) or the transoid (φ=180°) conformations.

## Cambridge Structural Database (CSD) analysis: Conformational variability in compounds with diacetylenic [–C≡C–C≡C–] spacer

CSD (ConQuest *v1.15; update Feb, 2013*) analysis was carried out for the symmetrically 1, 6 disubstituted hex–2,4–diyne structures with various substituent groups at the two ends of the diacetylenic spacer unit. In order to probe the most preferred packing patterns in this class of compounds, the entries were selected with the substituent group (R) ranging from a simple methyl group to the relatively bulkier polysubstituted groups.

### Filters used during CSD search

1. 3D coordinates determined
2. No errors
3. No powder structures
4. No repeated structure
5. Not disordered
6. Not polymeric
7. No cyclic compounds
8. No Hydrates and Solvates
9. Single component structures (No cocrystals)
10. Only organics (No Coordination compounds)

The filters 6–10 are crucial in order to precisely evaluate the orientational preferences of the substituent groups across the diacetylenic spacer [R–$H_2$C–C≡C–C≡C–$CH_2$–R] without any influence of external factors such as polymerization, cyclization, crystallization with other molecules (coformers), formation of solvates/hydrates and coordination through triple bonds.
The CSD analysis with above restrictions resulted in 79 hits. The adoption of a centrosymmetric anti molecular conformation (φ = 180 °) prevails in about 62 % (49 out of 79 hits) of the structures whereas, no specific conformational preferences have been observed for remaining 38 % structures. Table S3 and figure S7 provide an overall distribution of torsions observed in the CSD analysis.

**Table S3** CSD refcodes for the entries with their respective crystallographic and conformational features.

| Sr. No. | Refcode | Space Group | Z Value | Z Prime | Torsion angle, φ (°) |
|---|---|---|---|---|---|
| 1 | BASBUT | P–1 | 2 | 1 | 140.67 |
| 2 | BASLUC | C2/c | 8 | 1 | 169.46 |
| 3 | BASLUC01 | C2/c | 8 | 1 | 169.82 |
| 4 | BASMAJ | P21/c | 2 | 0.5 | 180 |
| 5 | BASMAJ01 | P21/a | 2 | 0.5 | 180 |
| 6 | BELBAV01 | P21/c | 2 | 0.5 | 180 |

| | | | | | |
|---|---|---|---|---|---|
| 7 | BICROU | P–1 | 1 | 0.5 | 180 |
| 8 | BUGMUL | P–1 | 1 | 0.5 | 180 |
| 9 | CAFMOL[#] | P–1 | 3 | 1.5 | 180 |
| 10 | | | | | 173.53 |
| 11 | CECDIX | P–1 | 2 | 1 | 162.54 |
| 12 | CISKAQ | P–1 | 1 | 0.5 | 180 |
| 13 | COYLUX | P21/a | 2 | 0.5 | 180 |
| 14 | COYMAE | P21/c | 2 | 0.5 | 180 |
| 15 | CUVJIM | Pbca | 4 | 0.5 | 180 |
| 16 | DEMXIC | P21/n | 2 | 0.5 | 180 |
| 17 | DISZUA | C2/c | 8 | 1 | 177.17 |
| 18 | DOGZEE | P21/c | 4 | 1 | 59.84 |
| 19 | DOHZAB | P21/c | 4 | 1 | 109.21 |
| 20 | DOHZAB01 | P21/c | 4 | 1 | 110.14 |
| 21 | DOHZAB02 | P21/n | 4 | 1 | 108.98 |
| 22 | DUKKUP | P–1 | 1 | 0.5 | 180 |
| 23 | DUKLAW | P21/n | 2 | 0.5 | 180 |
| 24 | EDILEI | P21/a | 2 | 0.5 | 180 |
| 25 | EDILIM | P21/n | 2 | 0.5 | 180 |
| 26 | EMICIN | P21/c | 2 | 0.5 | 180 |
| 27 | FAQPAO | P21/c | 4 | 1 | 6.84 |
| 28 | FAQPES | Cn | 4 | 1 | 2.09 |
| 29 | FUPFUR | P–1 | 2 | 1 | 179.01 |
| 30 | GAGBAT | C2/c | 4 | 0.5 | 145.24 |
| 31 | HDYNTS01 | P21/c | 4 | 1 | 180 |
| 32 | HDYNTS02 | P21/c | 2 | 0.5 | 180 |
| 33 | HEXYBS | P–1 | 1 | 0.5 | 180 |
| 34 | HEZPAE | C2/c | 4 | 0.5 | 30.74 |
| 35 | HOLMUQ | P–1 | 1 | 0.5 | 180 |
| 36 | HXDYFS01 | P21/c | 2 | 0.5 | 180 |
| 37 | HXDYNB | P21/c | 2 | 0.5 | 180 |
| 38 | HXDYNB01 | P21/c | 2 | 0.5 | 180 |
| 39 | HXDYNB02 | P21/n | 2 | 0.5 | 180 |
| 40 | HXDYTU | C2/c | 4 | 0.5 | 180 |
| 41 | HXYMBS | P–1 | 1 | 0.5 | 180 |
| 42 | HXYNPS | P21/n | 2 | 0.5 | 180 |
| 43 | JATCUC | P21/n | 2 | 0.5 | 180 |
| 44 | KENFAK | P21/c | 2 | 0.5 | 180 |
| 45 | KOGWUY | Pbca | 4 | 0.5 | 180 |
| 46 | LOTZEZ* | P–1 | 2 | 1 | 92.57 |

| | | | | | |
|---|---|---|---|---|---|
| 47 | LOTZEZ01* | P21/c | 2 | 0.5 | 180 |
| 48 | LOTZID | P21/c | 2 | 0.5 | 180 |
| 49 | LOTZOJ | P–1 | 1 | 0.5 | 180 |
| 50 | LOTZUP | P–1 | 2 | 1 | 90.9 |
| 51 | NUNMEO | P21/c | 2 | 0.5 | 180 |
| 52 | OCDYDL | P21/c | 4 | 1 | 93.39 |
| 53 | OCTTLS | P–1 | 1 | 0.5 | 180 |
| 54 | PIWDUV | C2/c | 4 | 0.5 | 180 |
| 55 | PIWDUV01 | C2/c | 4 | 0.5 | 180 |
| 56 | POXHYN10 | Pcab | 4 | 0.5 | 180 |
| 57 | POXHYN11 | P21/c | 2 | 0.5 | 180 |
| 58 | QEVGAA | P21/c | 2 | 0.5 | 180 |
| 59 | QOHXER | P21/c | 4 | 1 | 108.88 |
| 60 | SADPAQ | P21/n | 2 | 0.5 | 180 |
| 61 | SADPEU | P21/n | 4 | 1 | 137.14 |
| 62 | SADPIY | P21/n | 4 | 1 | 161.87 |
| 63 | SADPOE | P–1 | 1 | 0.5 | 180 |
| 64 | SADPUK | P–1 | 2 | 1 | 122.11 |
| 65 | SADQAR | P–1 | 1 | 0.5 | 180 |
| 66 | SAXGUT | C2/c | 4 | 0.5 | 180 |
| 67 | SOPMEP | P–1 | 1 | 0.5 | 180 |
| 68 | TACKUD | P–1 | 2 | 1 | 55.3 |
| 69 | TAJVUW | C2/m | 2 | 0.25 | 180 |
| 70 | TAJWAD | C2/c | 4 | 0.5 | 67.69 |
| 71 | TCDUAC | P21/a | 2 | 0.5 | 180 |
| 72 | VASTOY | P21/c | 4 | 1 | 142.23 |
| 73 | VAZRIX* | P21/n | 2 | 0.5 | 180 |
| 74 | VAZRIX01* | P21/n | 4 | 1 | 55.61 |
| 75 | VUKVAZ | P–1 | 2 | 1 | 70.66 |
| 76 | VUYTOY | C2/c | 4 | 0.5 | 125.02 |
| 77 | YAFGUI | P–1 | 1 | 0.5 | 180 |
| 78 | ZESCEF | C2/c | 4 | 0.5 | 153.86 |
| 79 | ZIPBOP | P–1 | 2 | 1 | 77.87 |

[#] Two different conformations (φ= 180° and φ=173.53°) of a molecule have been observed in a same crystal with one (φ=173.53°) and a half (φ= 180°) molecule in the asymmetric unit, Z' = 1.5.

*Two polymorphs of a compound (Conformational Polymorphism) have been observed with different molecular conformations in the crystal structures.

These cases clearly indicate the conformational flexibility of such symmetrically 1, 6 disubstituted hex–2,4–diynes which could be tuned during crystallization experiments.

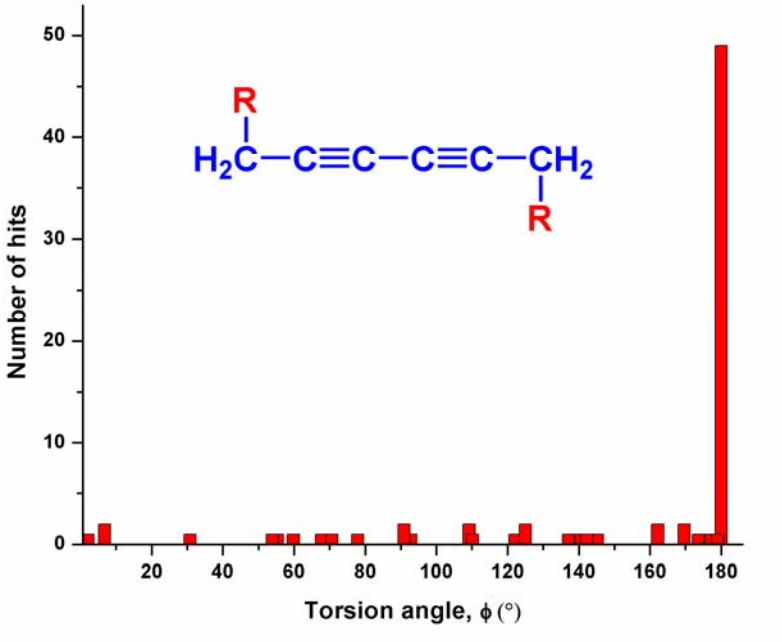


**Figure S7:** Plot of number of hits (n) versus the torsion angle (ϕ) for diacetylene spaced symmetrically 1, 6 disubstituted hex–2,4–diyne structures obtained in the CSD analysis [Total no. of hits=79; hits with ϕ=180º, 49].